ENGINEERING TRANSACTIONS • *Engng. Trans.* • **61**, 4, 301–315, 2013
Polish Academy of Sciences • Institute of Fundamental Technological Research (IPPT PAN)
National Engineering School of Metz (ENIM)

Method for Determination of the Dynamic Elastic Modulus for Composite Materials

Abdellah MASSAQ[1), 2)], Alexis RUSINEK[3)], Maciej KLÓSAK[4), 5)]

[1)] *Ecole Nationale des Sciences Appliquées*
Avenue Abdelkrim Khattabi, 40000, Guéliz-Marrakech, Maroc

[2)] *IbnoZohr University, Faculty of Sciences Agadir*
BP. 8106 Quartier Dakhla, Agadir, Morocco; e-mail: a.massaq@uiz.ac.ma

[3)] *National Engineering School of Metz ENIM*
Laboratory of Mechanics, Biomechanics, Polymers and Structures – LaBPS, EA 4632
1 route d'Ars Laquenexy, CS 65820 57078 METZ Cedex 3, France; e-mail: rusinek@enim.fr

[4)] *Universiapolis, Ecole Polytechnique d'Agadir*
Bab Al Madina, Qr Tilila, Agadir, Morocco; e-mail: klosak@e-polytechnique.ma

[5)] *The State School of Higher Professional Education in Kalisz*
4 Nowy Swiat Street, 62-800 Kalisz, Poland

Majority of polymer matrix composite materials, a marked viscoelastic behavior and faculties of dissipation of energy, it thus proves necessary to know the viscoelastic properties, as the dynamic Young modulus. In this work, we will present a new experimental technique for determining the dynamic elastic modulus at high strain rates of polymer matrix composites materials by a statistical method demanding a large number of tests. This new technique is based on the split Hopkinson pressure bar. Further, we study the effect of strain rate on dynamic elastic modulus of a woven Polyamid 6 – glass fibre reinforced.

Key words: composite, dynamic Young modulus, Hopkinson bar, high strain rate.

1. Introduction

Elastic constants of materials have a great importance, both for engineering practice and research, because they describe a mechanical behavior of materials. Contrary to static loading for which these constants are clearly defined, the dynamic loading causes some difficulties in their determination. For a long time, dynamic values were derived from static ones. Then they were measured using visco-acoustic methods or ultrasounds [1–5]. However, those methods do not allow to cover a large range of stresses and they give a complex rigidity matrix

only at high frequencies. In order to determine a dynamic elastic modulus, some authors [5] directly use a linear part of stress-strain curve.

Our technique is based on the Hopkinson bar in compression [6, 7] which covers a large range of stresses for a range of very low frequencies. The use of the Hopkinson bar has become the most adopted and widely used method for determination of dynamic properties of composite materials.

2. Material and measurement techniques

2.1. Material

The tested material is a composite made of armor tissue of equilibrate glass fiber and the matrix is composed of Polyamide 6 (PA6). The tests have been carried out on cylindrical specimens, loaded in three compression directions **L1**, **L2** and **T** (Fig. 1).

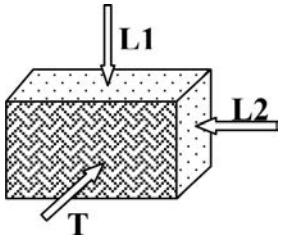

Fig. 1. Compression directions. Direction **T**: compression perpendicular to fibers, directions **L1** and **L2**: compression in the fibers principal direction.

2.2. Measurement of the wave propagation velocity in the composite PA6/glass

2.2.1. Measurement techniques. The technique allows to determine a propagation velocity of an elastic wave through the material cross-section. It uses Hopkinson bars for short-time loading $0 < t < 2\Delta t_s$, where Δt_s is transmission time of the elastic wave in the material [7]. This enables to determine a dynamic longitudinal elastic modulus for stresses close to zero:

$$E_d = \lim_{\sigma \to 0} \left(\frac{\partial \sigma}{\partial \varepsilon} \right)_{\sigma}. \tag{2.1}$$

This is a gradient at a point of the characteristic stress-strain curve which is demonstrated in Fig. 2 for the zero point.

The principle of the method is shown in Fig. 3. It consists on determination of time necessary for a wave to pass through the composite specimen. This measurement of time Δt_s is performed in two steps. First, an analysis of the oscillogram of an empty test is made, that means without a specimen and with two bars in contact (Fig. 3a). It allows to obtain the time Δt_0 necessary for the

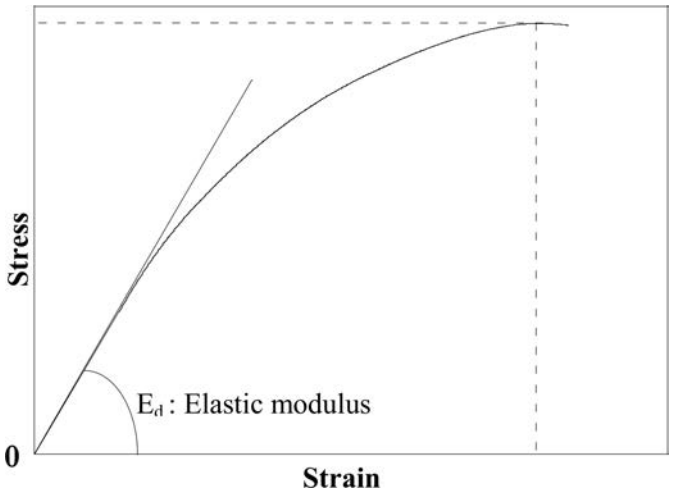

FIG. 2. Representation of the dynamic elastic modulus.

transmission of the elastic wave between the gauges T_1 and T_2. Second, another test is realized in which the specimen of the length l is introduced between two bars which is shown in Fig. 3b. In this case, we measure the time Δt of the elastic wave transmission between the gauges T_1 and T_2 of the complete system bar-specimen-bar.

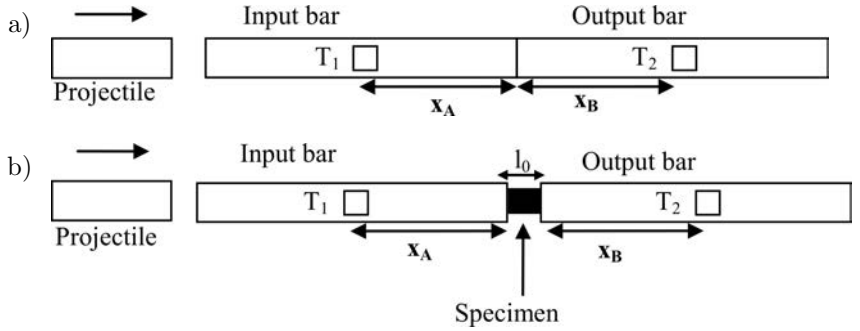

FIG. 3. a) Calibration of the set-up without specimen to define the characterisitic time; b) Principle of the method for determination of transmission time of the elastic wave in the specimen.

Thereby, the difference between these two time intervals is equal to the propagation time Δt_s of the wave through the composite specimen. No loading is applied. We have then:

$$\Delta t_s = \Delta t - \Delta t_0 \,. \tag{2.2}$$

The velocity of the elastic wave in the bar is:

$$C_0 = \frac{x_A + x_B}{\Delta t_0} \,. \tag{2.3}$$

The celerity of wave propagation in the material is denoted by C_{os} and is given by:

$$C_{0s} = \left[\frac{l_0}{\Delta t_s}\right]_\sigma , \tag{2.4}$$

where l_0 is the specimen length and σ is the applied loading.

The propagation velocity of the longitudinal elastic wave is independent of a local velocity, this means the velocity of an element that transmits the wave. It only depends on elastic properties of the material and on temperature.

We have carried out an extended study to define conditions for founding experimental results which can be exploitable and with a minimum of the error level due to time dependence. The optimal specimen length of 16 mm has been adopted. In addition, for each specimen we have performed two test series. Each series is made of 100 tests. The first series permits to determine the mean value of $\overline{\Delta t}$ whereas the second one is for $\overline{\Delta t_0}$ evaluation. The tests with and without specimen have been mixed.

2.2.2. Results and discussion. The test results are presented in Figs. 4, 5 and 6. We have defined a basic time $\Delta t_b = 222$ μs, from which we obtain:

$$\Delta t_0 = \Delta t_0^* + \Delta t_b \quad \text{and} \quad \Delta t = \Delta t^* + \Delta t_b \, . \tag{2.5}$$

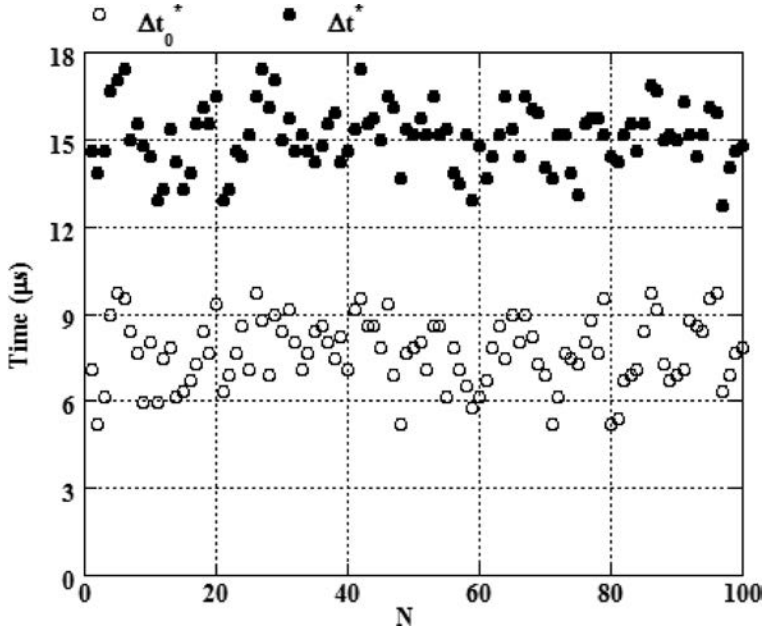

FIG. 4. Evolution of Δt^* and Δt_0^* as a function of the tests number; compression direction **T**.

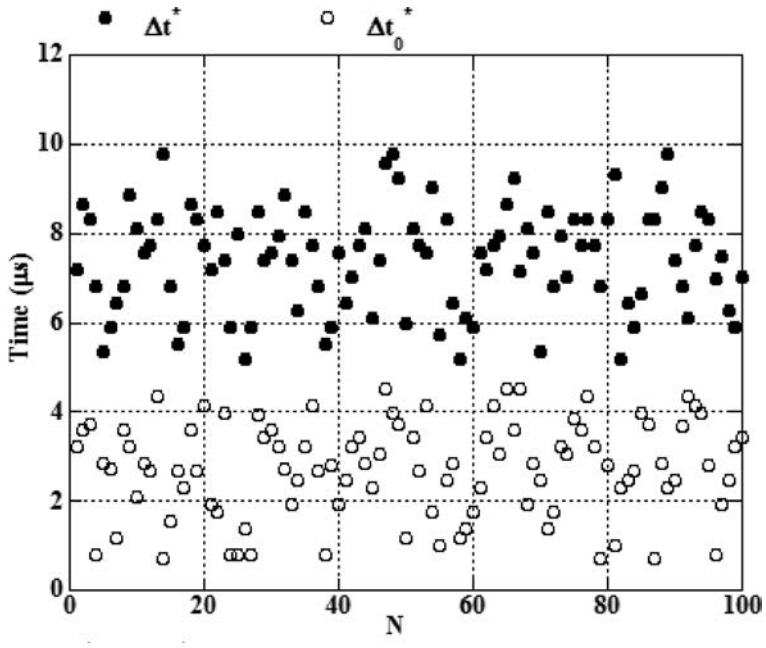

FIG. 5. Evolution of Δt^* and Δt_0^* as a function of the tests number; compression direction **L1**.

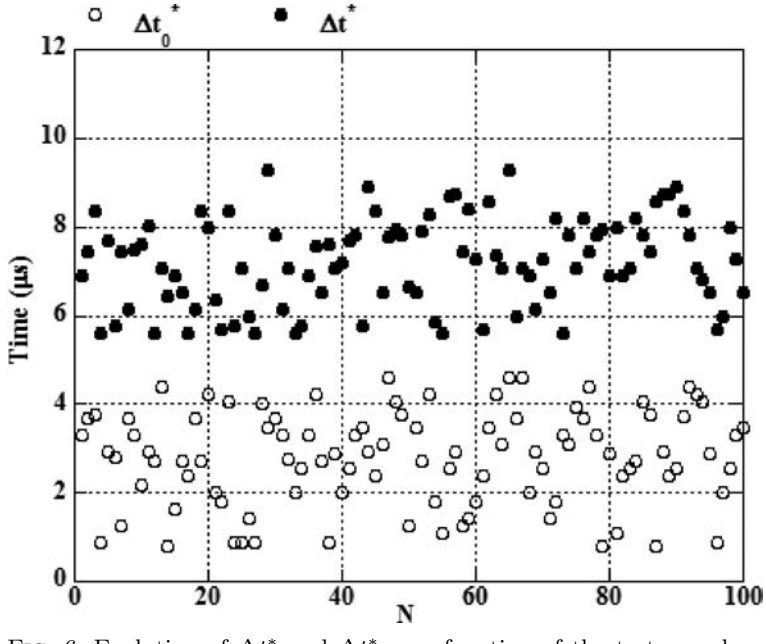

FIG. 6. Evolution of Δt^* and Δt_0^* as a function of the tests number; compression direction **L2**.

In this configuration, Δt_0^* and Δt^* represent new time scales. In order to avoid any risk of cracking in the material core, we have decided to perform tests at very low strain rates from 0.8 s^{-1} to 3 s^{-1}. The large number of tests has permitted to realize a static analysis of Δt and Δt_0 as well as a precise calculation of the wave transmission in our composite material.

The frequencies related to three compression directions given as a function of time Δt and Δt_0 can be presented by the histogram as it is shown in Figs. 7, 8 and 9. The relative frequencies distribution allows to carry out first observations on the evolution of time of the elastic wave propagation, but it also gives a first representation of the cumulative probability. The matrix of this function i.e. a cumulative probability has a key role in the stochastic approach of design.

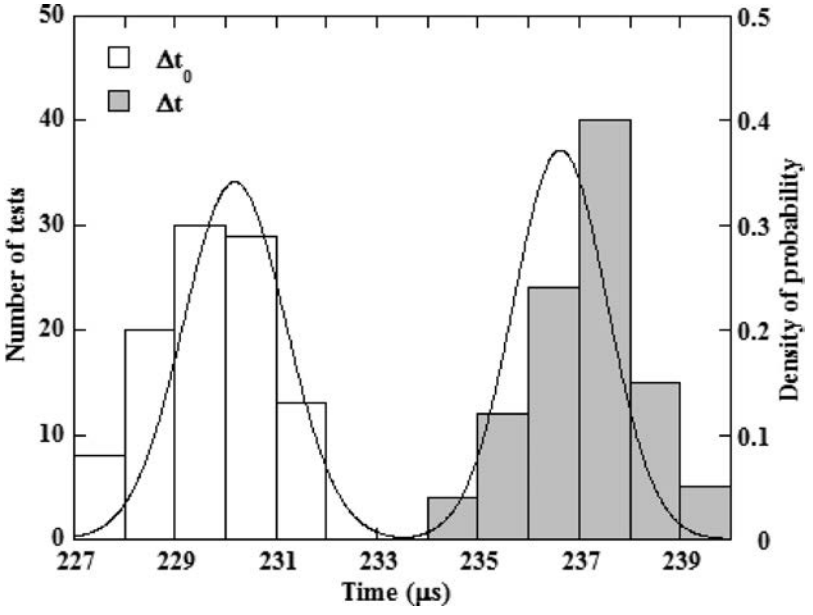

FIG. 7. Frequential distribution of Δt and Δt_0 represented in the form of histogram, adjusted by a normal distribution: compression direction **T**.

Table 1. Maximum relative frequencies and their classes for three compression directions.

	Compression direction					
	L1		**L2**		**T**	
Time	Δt_0	Δt	Δt_0	Δt	Δt_0	Δt
Class (μs)	[225–226]	[229–230]	[224–225]	[229–230]	[229–230]	[237–238]
Max. freq %	32	32	30	39	30	40

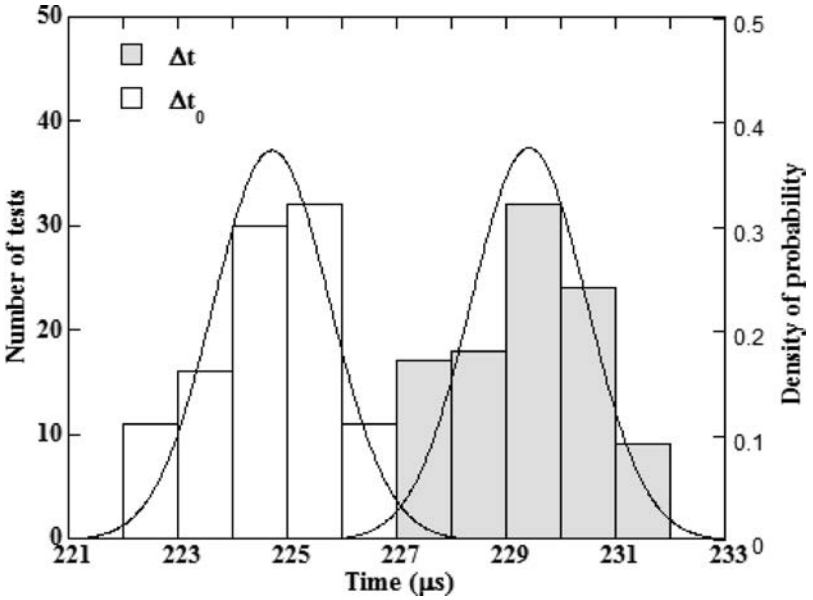

FIG. 8. Frequential distribution of Δt and Δt_0 represented in the form of histogram, adjusted by a normal distribution: compression direction **L1**.

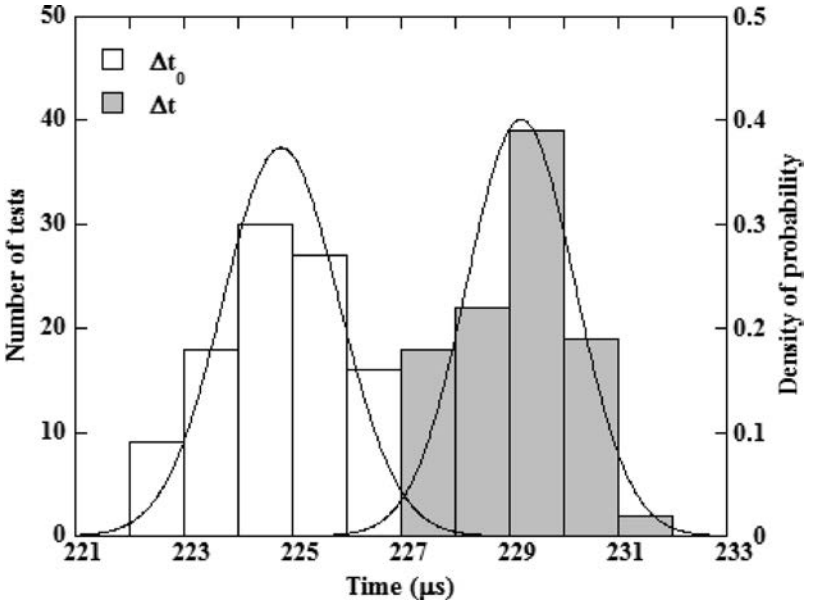

FIG. 9. Frequential distribution of Δt and Δt_0 represented in the form of histogram, adjusted by a normal distribution: compression direction **L2**.

2.2.3. Adjustment by the normal law. In order to perform an analysis based on a stochastic approach, it is fundamental to know a function of the density of

probability. This function can be expressed by the following formula:

$$p(\Delta t) = \left[\left(\frac{1}{S}\sqrt{2\pi}\right) \cdot \exp\left(-\frac{1}{2}\left(\frac{\Delta t - \overline{\Delta t}}{S}\right)^2\right)\right], \quad S > 0. \tag{2.6}$$

where Δt is a variable.

The mean time $\overline{\Delta t}$ and the interval of type S of this population is given by the following relations, respectively:

$$\overline{\Delta t} = \frac{1}{N}\sum_{i=1}^{N}(\Delta t)_i\,, \tag{2.7}$$

$$S = \left[\frac{1}{(N-1)}\sum_{i=1}^{N}(\Delta t - \overline{\Delta t})^2\right]^{1/2}, \tag{2.8}$$

where N represents the number of observations.

All the histograms obtained during the tests have been adjusted by the normal law described here above. In Table 2, we have reported the mean values $\overline{\Delta t_0}$ and $\overline{\Delta t}$ deducted from those histograms (Figs. 7, 8 and 9) after adjustment by the normal law.

The mean value of the wave passage through the specimen, described as $\overline{\Delta t_s}$, is defined by:

$$\overline{\Delta t_s} = \overline{\Delta t} - \overline{\Delta t_0}\,. \tag{2.9}$$

The celerity C_{0s} is deducted from the expression (2.4).

It is important to note that due to the use of the value of $\overline{\Delta t_0}$ we could evaluate the elastic wave.

Table 2. Mean values deducted through the normal law.

	Δt_0 (µs)	Δt (µs)	Δt_s (µs)	C_{0s} (mm/µs)
Compression direction **L1**	224.72	229.42	4.69	3.359
Compression direction **L2**	224.79	229.21	4.42	3.548
Compression direction **T**	229.67	237.11	7.44	2.346

2.2.4. Normality test using the Henry line. In order to validate the results obtained by the static analysis and then adjusted by the normal law, we have compared them with those adjusted by the method of Henry which is described in Saporta [8]. The latter consists on the graphical treatment of data. It enables to quickly verify whether a statistical distribution of a continuous variable resembles a normal distribution.

According to the method of Henry, if a variable $\overline{\Delta t}$ is a Gaussian one, for points $(\Delta t_i;\ U_i)$, where $U_i = (\Delta t_i - \overline{\Delta t})/S$, should be on the same line.

We can conclude from Fig. 10 that the points are aligned and the graphical adjustment using the method of Henry is satisfactory.

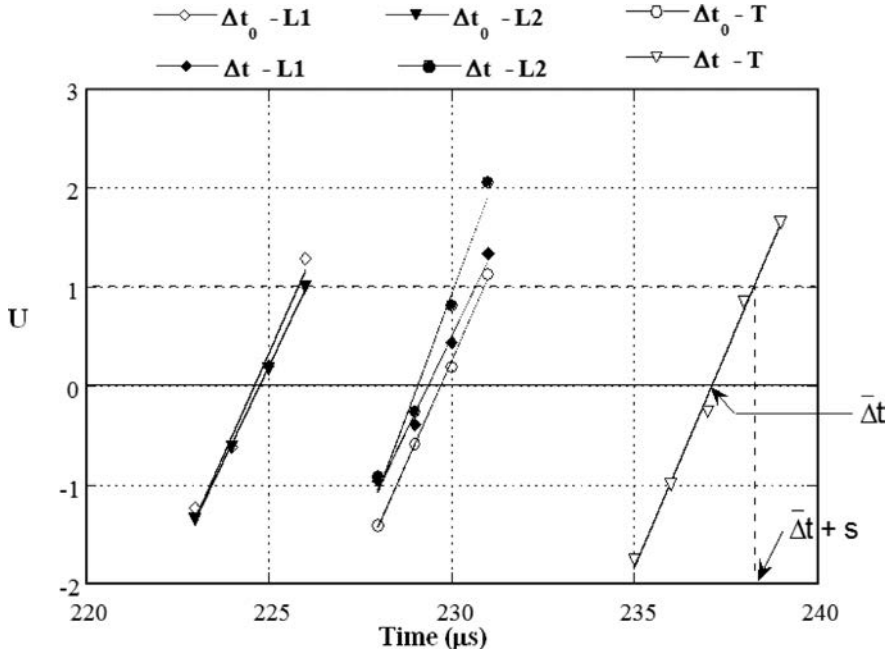

FIG. 10. Graphical adjustment to the law of Laplace-Gauss obtained for the compression directions **T**, **L1** and **L2**.

In Table 3, we have presented the theoretical Mean value ($\overline{\Delta t_0}$ and $\overline{\Delta t}$) and standard deviation S, calculated by the method of Henry, for three compression directions.

Table 3. Comparison: experiment vs. Henry's method.

		L1		**L2**		**T**	
		Δt_0	Δt	Δt_0	Δt	Δt_0	Δt
Henry's method	Standard deviation S	1.2000	1.3000	1.2888	1.0000	1.1889	1.1666
	Mean value (μs)	224.6	226.36	224.76	229.08	229.70	237.12
Experimental method	Standard deviation S	1.0671	1.1604	1.0671	0.9947	1.1686	1.0726
	Mean value (μs)	224.72	229.42	224.79	229.21	229.67	237.11

We have concluded that the graphical estimations of $\overline{\Delta t}$, $\overline{\Delta t_0}$ and S (standard deviation) differ slightly from the values $\overline{\Delta t_0}$, $\overline{\Delta t}$ and S determined through the described method (see Table 3).

From this comparative study, it appears the normal law is completely efficient to describe the frequential evolution of the elastic wave propagation time in the Hopkinson bar (with or without specimen). Finally, this adjustment method using the normal law has been adopted for all statistical analysis of our experimental results. In Fig. 11, we have presented the distribution functions of the variables Δt_0 and Δt for three tested compression directions. The functions are defined by the following expression:

$$P(\Delta t) = \int_{-\infty}^{+\infty} p(\Delta t)\,\mathrm{d}(\Delta t). \tag{2.10}$$

The probability density functions obtained in the analysis have a similar allure for all compression directions **L** or **T**.

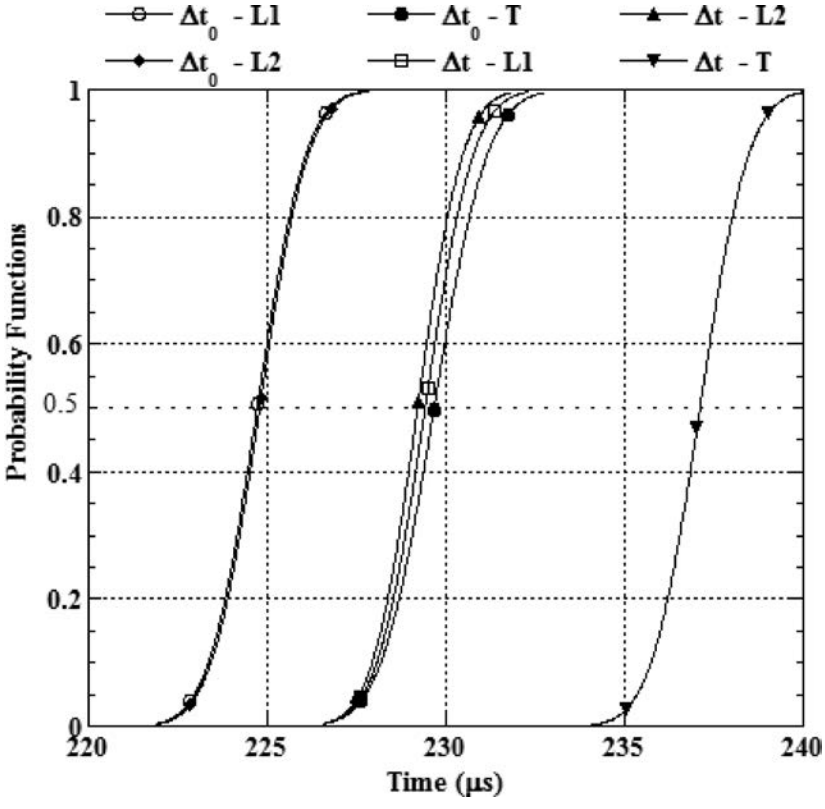

FIG. 11. Probability functions obtained for the compression directions **T**, **L1** and **L2**.

3. Dynamic elastic modulus

Whilst it can be easily demonstrated that for metallic materials the elastic modulus is practically constant for any strain rate (conservation of the static value), it is not the case for viscoplastic materials such as most of polymers or composite materials with the polymer matrix.

Under dynamic loading, the phenomena of rotation or slipping may change a molecular structure of the polymer matrix, both in the crystalline and amorphous phase [9]. This change in structure may result in a change of the Young modulus which is a physical value linked to the material structure, in particular to the molecular orientation [10]. This is why it becomes so important to estimate the Young modulus in dynamic conditions.

The instant dynamic elastic modulus E_d is given by:

$$E_d(\sigma) = \left(\frac{\partial \sigma}{\partial \varepsilon}\right)_{\sigma}; \qquad \sigma > 0. \tag{3.1}$$

For stresses close to zero, the wave celerity does not depend on its frequency [7], therefore E_d is reduced to:

$$E_d = \rho_0 C_{0s}^2, \tag{3.2}$$

where ρ_0 is the mean value of the specimen density of the composite material used in the tests. For short loading intervals of time, $0 < t < 2\Delta t_s$, the celerity $C_{0s}(\sigma)$ is determined by:

$$\left(\frac{\partial \sigma}{\partial \varepsilon}\right)_{\sigma} = \rho_0 C_{0s}^2(\sigma). \tag{3.3}$$

The stress-strain relation is defined by the following equation:

$$\varepsilon = \frac{1}{\rho_0} \int_0^{\sigma} \frac{\mathrm{d}\sigma}{C_{0s}^2(\sigma)}; \qquad \sigma = \text{constant}. \tag{3.4}$$

The wave celerity $C_{0s}(\sigma)$ is a slightly decreasing function of σ.

In Table 4, we have presented the values of the dynamic elastic modulus calculated by Eq. (3.2) for three compression directions.

Table 4. Dynamic elastic modulus for three compression directions.

Compression directions	**L1**	**L2**	**T**
E_d (MPa)	20691	23085	10098

4. Impact of strain rate on the elastic modulus

In order to study the impact of strain rate on the elastic modulus, the compression tests in quasi-static conditions have been carried out using a hydraulic machine (Zwick REL). The compression dynamic tests have been performed with the Hopkinson bar system. The range of strain rates: 10^{-5} s^{-1} to 2300 s^{-1}.

Three specimens have been used for each test condition. Figures 12, 13, and 14 present a synthesis of stress-strain curves for the composite PA6/glass, loaded in the parallel and perpendicular direction to fibers.

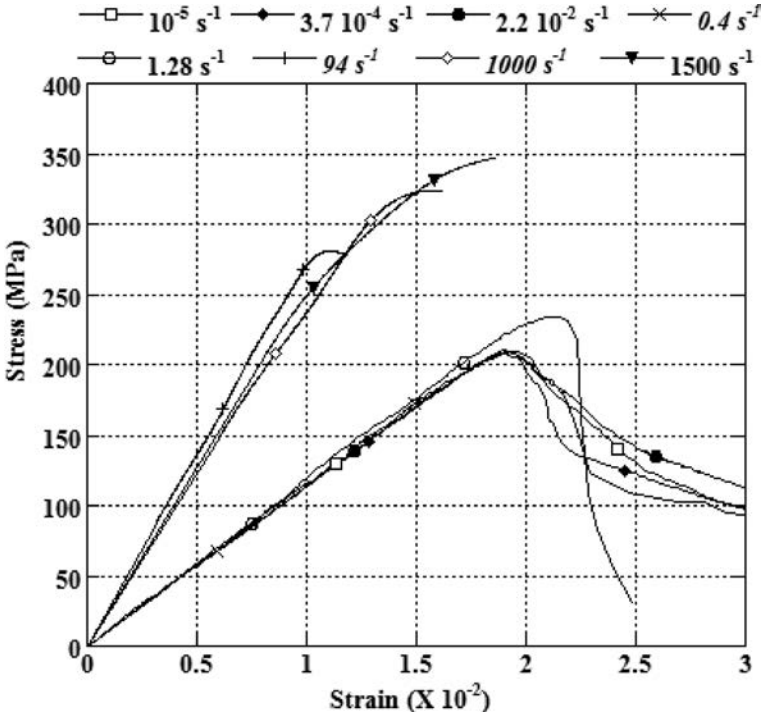

Fig. 12. Stress-strain curve at different strain rates, compression direction **L1**.

The dynamic modulus is higher that the static modulus obtained during the quasi-static compression tests. Table 5 reveals this difference which proves a high viscosity of the matrix.

Table 5. Dynamic elastic modulus for three compression directions.

Compression directions	E_s (MPa)	E_d/E_s	$(E_d - E_s)/E_s$ (%)
L1	11281	1.8	83.4
L2	11466	2.0	101.3
T	5265	1.9	91.8

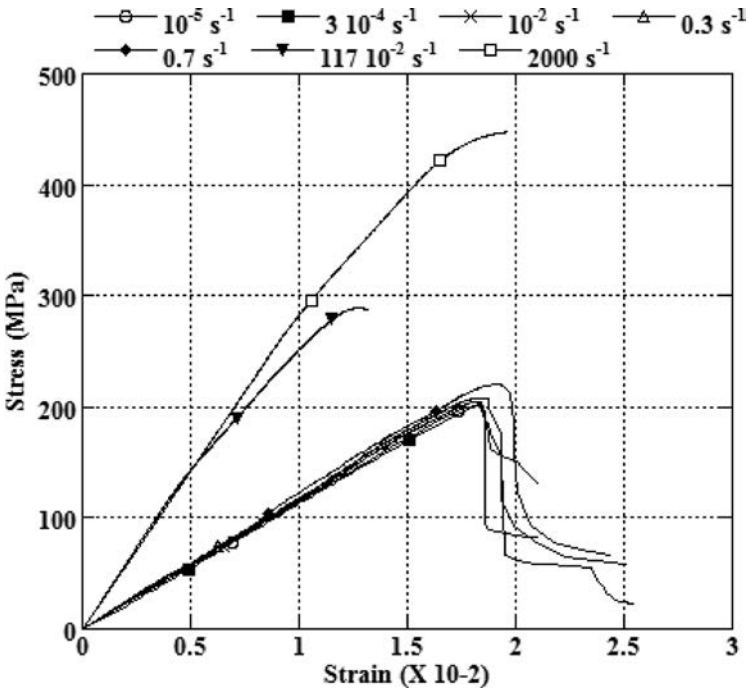

FIG. 13. Stress-strain curve at different strain rates, compression direction **L2**.

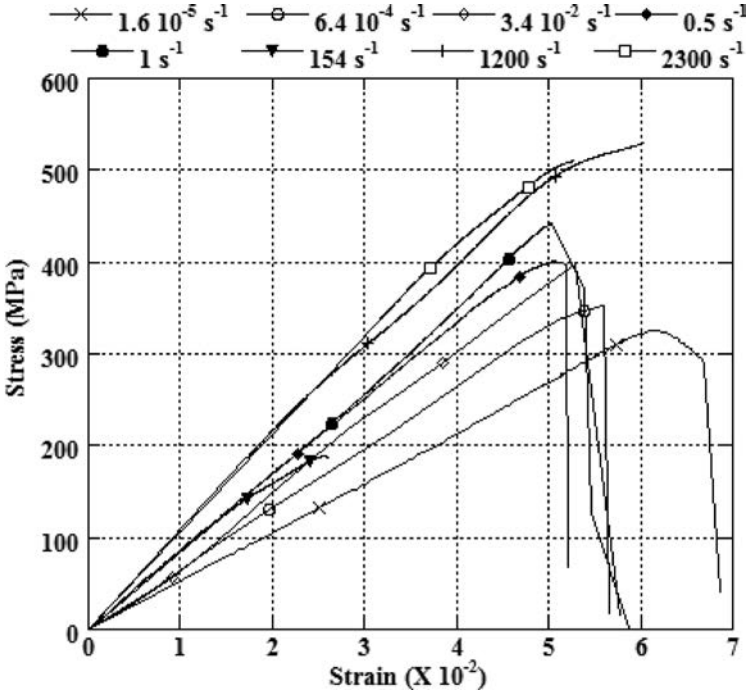

FIG. 14. Stress-strain curve at different strain rates, compression direction **T**.

Figure 15 shows the elastic modulus is sensitive to the strain rate because the values obtained in dynamic tests are higher that those form quasi-static ones. As far as compression in fibers direction is concerned, we can also observe a slight strain rate sensitivity for quasi-static loadings. On the other hand, the modulus increases linearly above $\dot{\varepsilon} = 1\ \mathrm{s}^{-1}$. In case of the compression direction **T**, the elastic modulus seems to vary linearly as a function of log for both ranges of strain rates (quasi-static and dynamic). A linear correlation leads to the following equation:

$$E_T = E_0 + \beta \log(\dot{\varepsilon}/\dot{\varepsilon}_0). \tag{4.1}$$

For $\dot{\varepsilon}_0 = 1\ \mathrm{s}^{-1}$, the quasi-static modulus in the compression direction **T**, $E_0 = 8577.7$ MPa, β is the sensitivity coefficient of the elastic modulus to the strain rate, $\beta = 673.41$.

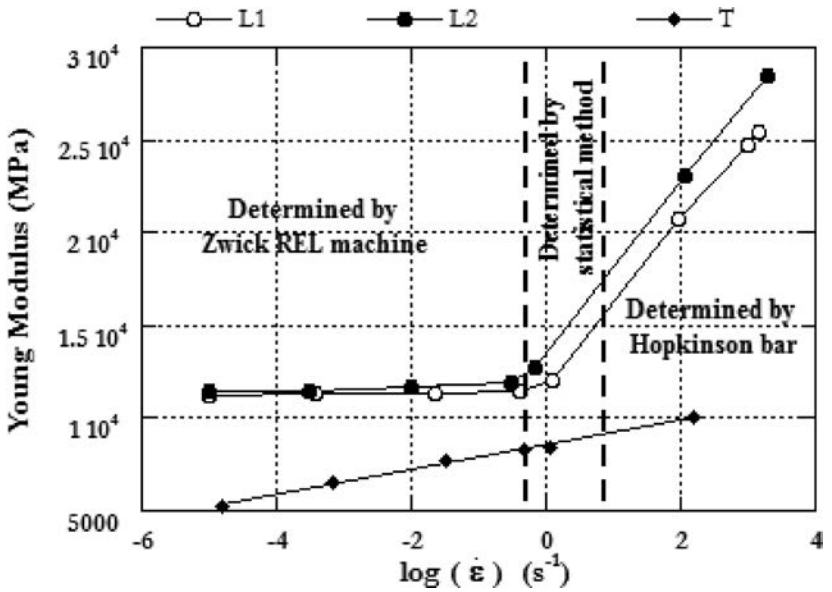

FIG. 15. Impact of the strain rate on the elastic modulus.

5. Conclusions

From the tests obtained, we can conclude and confirm the Hopkinson bar system enables to measure the wave propagation velocity in composite materials and calculate dynamic elastic modulus. In contrast to acoustic methods, this technique allows for determination of the elastic modules in the large range of stresses and at very low frequencies.

This conclusion opens a perspective to evaluate all dynamic elastic parameters (ν, G and E) for viscoelastic materials of a brittle or semi-brittle nature.

References

1. Olsen C., Fabricius L. Ida., Krogsboll A., Prasad M., *Static and dynamic Young's Modulus for Lower Cretaceous chalk. A low frequency scenario*, AAPG International Conference, Cancun, Mexico, 24-27, October 2004.
2. Olsen G.T., Wolfenden A., Hebsur M.G., *Experimental Investigation of the Dynamic Elastic Modulus and Vibration Damping in $MoSi_2$-30%Si_3N_4 as a Function of Temperature*, Journal of Materials Engineering and Performance, **9**, 1, 116–119, 2000.
3. Srikanath N., Saravanaranganathan D., Gupta M., Lu L., Lai M.O., *Modelling and determination of dynamic elastic modulus of magnesium based metal matrix composites*, Materials Science and Technology, **16**, 3, 309–314, 2000.
4. Zheng. L., Sharon Huo X., Yuan Y., *Experimental investigation on dynamic properties of rubberized concrete*, Construction and Building Materials, **22**, 939–947, 2008.
5. Tarfaoui M., Choukri S., Neme A., *Effect of fibre orientation on mechanical properties of the laminated polymer composites subjected to out-of-plane high strain rate compressive loadings*, Composites Science and Technology, **68**, 2, 477–485, 2008.
6. Klepaczko J.R., *The modified Split Hopkinson Bar*, Theoretical and Applied Mechanics, **4**, 479–491, 1971.
7. Klepaczko J.R., *Quasi-static and Dynamic Compression Behavior of Coal*, Technical Report No. 1, Dept. of Mech. Engng., The University of Manitoba, Winnipeg, 1982.
8. Saporta G., *Probabilités analyse des données et statique*, Ed. Technip, Paris, 1990.
9. Vermeulen B., Gueguen V., Bergé F., Perring F., Lam T.M., Reffo G., *Résistance ŕ l'impact des matériaux composites ŕ base de tissus de polyéthylčne haute performance, polyaramide et verre*, Composites, **19**, 53–57, 1997.
10. Word I.M., *Mechanical properties of solid polymers*, Ed. Wiley, London, 1983.

Received November 9, 2013; revised version December 22, 2013.